



Association between As and Cu renal cortex accumulation and physiological and histological alterations after chronic arsenic intake

Paolo N. Rubatto Birri^a, Roberto D. Pérez^{b,c}, David Cremonuzzi^d, Carlos A. Pérez^e, Marcelo Rubio^{b,c}, Guillermina A. Bongiovanni^{c,f,*}

^a Instituto de Biología Celular, Facultad de Ciencias Médicas (FCM), Universidad Nacional de Córdoba (UNC), Ciudad Universitaria, Córdoba, Argentina

^b Facultad de Matemática, Astronomía y Física (FAMAF-UNC), Ciudad Universitaria, Córdoba, Argentina

^c Consejo Nacional de Investigaciones Científicas y Tecnológicas (CONICET), Buenos Aires, Argentina

^d Cátedra Anatomía Patológica, Hospital Nacional de Clínicas (FCM-UNC), Córdoba, Argentina

^e Laboratório Nacional de Luz Síncrotron (LNLS), Linha D09B-XRF, Campinas SP, Brazil

^f Laboratorio de Investigaciones Bioquímicas, Químicas y de Medio Ambiente (LIBIQUIMA), Consejo Nacional de Investigaciones Científicas y Tecnológicas (CONICET), Universidad Nacional del Comahue, Buenos Aires 1400, CP 8300 Neuquén, Argentina

ARTICLE INFO

Article history:

Received 25 March 2009

Received in revised form

24 August 2009

Accepted 8 September 2009

Available online 18 February 2010

Keywords:

Hydroarsenicism
As accumulation
Cu accumulation
SR- μ XRF
As–Cu interaction

ABSTRACT

Arsenic (As) is one of the most abundant hazards in the environment and it is a human carcinogen. Related to excretory functions, the kidneys in humans, animal models or naturally exposed fauna, are target organs for As accumulation and deleterious effects. Previous studies carried out using X-ray fluorescence spectrometry by synchrotron radiation (SR- μ XRF) showed a high concentration of As in the renal cortex of chronically exposed rats, suggesting that this is a suitable model for studies on renal As accumulation. This accumulation was accompanied by a significant increase in copper (Cu) concentration. The present study focused on the localization of these elements in the renal cortex and their correlation with physiological and histological As-related renal effects. Experiments were performed on nine male Wistar rats, divided into three experimental groups. Two groups received 100 μ g/ml sodium arsenite in drinking water for 60 and 120 consecutive days, respectively. The control group received water without sodium arsenite (< 50 ppb As). For histological analysis, 5- μ m-thick sections of kidneys were stained with hematoxylin and eosin. Biochemical analyses were used to determine concentrations of plasma urea and creatinine. The As and Cu mapping were carried out by SR- μ XRF using a collimated white synchrotron spectrum (300 μ m \times 300 μ m) on kidney slices (2 mm thick) showing As and Cu co-distribution in the renal cortex. Then, renal cortical slices (100 μ m thick) were scanned with a focused white synchrotron spectrum (30 μ m \times 30 μ m). Peri-glomerular accumulation of As and Cu at 60 and 120 days was found. The effects of 60 days of arsenic consumption were seen in a decreased Bowman's space as well as a decreased plasma blood urea nitrogen (BUN)/creatinine ratio. Major deleterious effects; however, were seen on tubules at 120 days of exposition. This study supports the hypothesis that tubular accumulation of As–Cu may have some bearing on the arsenic-associated nephrotoxicological process.

© 2010 Elsevier Inc. All rights reserved.

1. Introduction

Arsenic (As) is one of the most abundant hazards in the environment and millions of people in several areas of world have high exposure to arsenic from naturally contaminated drinking water. Prolonged ingestion of arsenic-contaminated water may result in the manifestations of toxicity in practically all systems of

the body (hydroarsenicism) (Yoshida et al., 2004; Tapio and Grosche, 2006). Because of its ability to reabsorb and accumulate heavy metals, the kidney is the first target organ of arsenic toxicity (Pomroy et al., 1980; Parrish et al., 1999; Schnellmann and Kelly, 1999; Pérez et al., 2006a,b; ATSDR, 2007). Cortical necrosis, chronic renal insufficiency, acute renal failure and renal tumors are not uncommon in As-exposed humans (Gerhardt et al., 1978; National Research Council (NRC), 1999; Meliker et al., 2007; Sasaki et al., 2007). The tubular cells of the kidney are particularly vulnerable due to their disproportionate exposure to circulating chemicals and transport processes that result in high intracellular concentrations. Arsenic-associated oxidative stress, with both lipid peroxidation and protein oxidation, has been shown to

* Corresponding author at: Laboratorio de Investigaciones Bioquímicas, Químicas y de Medio Ambiente (LIBIQUIMA), Consejo Nacional de Investigaciones Científicas y Tecnológicas (CONICET)-UE, Universidad Nacional del Comahue, Buenos Aires 1400, CP 8300 Neuquén, Argentina.

E-mail address: gbongiovanni@conicet.gov.ar (G.A. Bongiovanni).

contribute to renal cell injury (Bongiovanni et al., 2007; Meliker et al., 2007; Soria et al., 2008). In many cases mitochondria are a critical target and the lack of adenosine triphosphate (ATP) leads to cell injury due to the dependence of renal function on aerobic metabolism. Following exposure to arsenic, those cells sufficiently injured die by one of two mechanisms, apoptosis or necrosis, which lead to the loss of tubular epithelial cells, tubular obstruction, “backleak” of the glomerular filtrate and a decreased glomerular filtration (Schnellmann and Kelly, 1999; Peraza et al., 2006). Furthermore, oral administration of inorganic arsenic has been shown to lead to an accumulation of arsenic and copper in the kidneys of several animal species (Hunder et al., 1999; Wang et al., 2006; Pérez et al., 2006b). Besides As, additional Cu accumulation may therefore be critical for that organ. Although the kidney is a target for the accumulation and toxicity of arsenic, little is known about arsenic–copper distribution or correlated effects in this organ. Since As and Cu nephrotoxicity had been extensively demonstrated, the spatial distribution or variation of As and Cu concentration in specific functional structures after inorganic arsenic exposure, is of critical importance. Furthermore, the correlation of specific changes in element concentrations with histological evidence of injury and metabolic disturbances could throw light on the arsenic-related toxicological processes. Consistent chemical analyses, such as atomic absorption spectroscopy and inductively-coupled plasma atomic emission spectroscopy, have been available for decades to quantify major and trace elements in biological samples. However, since these methodologies previously require acid digestion, determination of the spatial distribution or variation of element concentrations in specific functional structures is difficult. X-ray fluorescence spectrometry using synchrotron radiation (SR-XRF) is a high-sensitivity and non-destructive method for multi-element determinations in different matrices that enables quantitative study of trace constituents in biological and non-biological samples with a limit of detection of around 10 ppb for many elements (Figueroa and Bongiovanni, 2008; Pérez et al., 2006a). A privileged alternative, the microbeam method (SR- μ XRF), through the intrinsic characteristics of SR, is able to perform multi-element spectrochemical analysis with spatial resolution on the micrometer scale. Using this methodology, our recent results had provided experimental evidence that arsenic is not homogeneously distributed in all target organs (Pérez et al., 2006a). The spatial distribution of elements was determined by SR- μ XRF in the Brazilian Synchrotron Light Laboratory (LNLS). Arsenic was accumulated in the renal cortex and whole liver, while a weak signal was seen in the brain cortex and whole pancreas (Pérez et al., 2006b; Rubatto Birri et al., 2007; Pérez et al., 2008; Rubio et al., 2008). Accumulation in the kidney was accompanied by an increase in cortico-renal Cu concentration (Pérez et al., 2006b).

The present study focused on the distribution of As and Cu in the renal cortex and their relation with the nephrotoxicological process in chronically arsenic-exposed rats. In order to provide greater precision in the analytical method, measured time was increased (40 s/step instead of 10). Additionally, histological and physiological data are incorporated to determine renal lesions. Treatment was also extended to 120 days and tissue-specific As and Cu localization was achieved using a focused white beam ($30\ \mu\text{m} \times 30\ \mu\text{m}$) instead of an orthogonal collimated white beam ($300\ \mu\text{m} \times 300\ \mu\text{m}$).

2. Materials and methods

2.1. Sample preparation

In order to minimize the gender and life cycle effects (Vahter et al., 2007) 50-day-old adult male Wistar rats of were included in each experiment. The animals were divided into three equal groups (three each). Two groups received

drinking water containing 100 ppm of NaAsO₂ (Sigma-Aldrich, Argentina) *ad libitum* for different periods of time. One group received treatment for 60 days and the other for 120 days. The remaining non-treated group was the control group and this did not receive arsenite in drinking water. Thus, the animals received 53 ppm inorganic As during 60 and 120 consecutive days (approximately 30% of their lifespan). Since many inhabitants of Argentina consume 2 ppm As in drinking water throughout their lives, this was considered an appropriate model for As accumulation studies.

The animals were provided with standard rodent food (GEPESA Grupo Pilar S.A. www.gepsa.com) *ad libitum*. The feed was analyzed by conventional X-ray fluorescence analysis (XRF). The copper concentration was 5 mg/kg, and no arsenic was detected. Certificated water (< 50 ppb As) supplied by Aguas Cordobesas S.A. (www.aguascordobesas.com.ar) was used as drinking water.

Blood of control as well as of As-treated animals was collected by tail venous puncture every 15 days starting at 0 time up to 60 days and serum was prepared. Blood urea nitrogen (BUN) and creatinine levels were assayed using kits for in vitro diagnosis from Wiener Laboratories (Argentina, www.wiener-lab.com.ar), according to manufacturer's instructions.

In order to minimize background As-hemoglobin, which could be occurring in rats, after the administration of the last arsenic dose, the animals were given a 1-day rest (without arsenite) and then were sacrificed under light ether anesthesia. The kidneys were dissected. One of them was fixed with 10% buffered formalin for 24 h and routinely processed for histological examination. Four non-consecutive sections of 5 μm were obtained by microtome and stained with hematoxylin and eosin (HE) for light microscopic examination. Pathological examinations were conducted “blind”. For Synchrotron microscopic X-ray fluorescence analysis (SR- μ XRF), the other kidney was snap frozen at $-80\ ^\circ\text{C}$. In order to obtain maps of element distribution, the kidneys were longitudinally cut in 2-mm-thick slices containing cortex, medulla and papilla. These slices were lyophilized and then fixed in acrylic resin for SR- μ XRF measurements using $300\ \mu\text{m} \times 300\ \mu\text{m}$ collimator. For element determination in the renal cortex, these were cut in 100- μm -thick slices by cryostat, and maintained in dry ice until SR- μ XRF measurement using a focused beam ($30\ \mu\text{m} \times 30\ \mu\text{m}$).

2.2. Instrumentation

Values of X-ray fluorescence intensities were obtained in the Synchrotron Light National Laboratory (Laboratório Nacional de Luz Síncrotron, LNLS) (Pérez et al., 1999). This is an international synchrotron research facility located in Campinas, Brazil. The energy of the electron bunch inside the storage ring reaches 1.37 GeV. A dipolar bending magnet – 1.65 T magnetic field intensity – accelerates the electrons emitting a photon spectrum with a critical energy of 2.08 keV. The photons are guided into the D009B beamline where the XRF set-up is placed. XRF measurements were performed by exciting the kidney slices pixel by pixel with a white synchrotron spectrum beam. To study kidney slices, the white beam was collimated by a pinhole giving a spatial resolution of $300\ \mu\text{m} \times 300\ \mu\text{m}$. A better spatial resolution of $30\ \mu\text{m} \times 30\ \mu\text{m}$ was obtained focusing the white beam with a tapered glass monocrapillary. The set-up with high spatial resolution was applied to perform more detailed analysis of fine renal cortical slices

Each sample was positioned in the image plane within an accuracy of 0.5 μm with a 3-axis (x,y,z) remote-controlled stage. A video microscope (magnification 500 \times) was used to spot the pixels of reference precisely in the incoming microbeam. XRF measurements were performed using a standard geometry (45–45 $^\circ$). The excitation beam was collimated by an orthogonal collimator ($300\ \mu\text{m} \times 300\ \mu\text{m}$). In this way, pixels of $300\ \mu\text{m} \times 300\ \mu\text{m}$ were obtained, keeping a high flux of photons on the sample. Optionally, this collimated beam could be focused on the sample up to pixels of $30\ \mu\text{m} \times 30\ \mu\text{m}$ by a tapered glass monocrapillary. This lens was mounted on a precision remote control stage which enabled its correct alignment. The fluorescence spectra were recorded with a Si(Li) detector of 165 eV FWHM at 5.9 keV in air atmosphere. It was set in the horizontal plane at 90 $^\circ$ to the incident beam to minimize scattering. K_{α} X-ray fluorescence intensity scanning was performed of one kidney slice (2 mm thick) from each group of rats in each experiment. The area selected for two-dimensional scanning (x;y) was a representative part of the kidney covering nearly 1/4 of the total sample, approximately. It contained the cortex, medulla and papilla. The counting live-time for each pixel ($300\ \mu\text{m} \times 300\ \mu\text{m}$) was 40 s/step, the step size was 300 μm in both directions and 3-D mappings were obtained (x–y elemental distribution vs. fluorescence intensity). For 2-D graphics, a transect line of twenty points was obtained by measuring K_{α} X-ray fluorescence intensity across pre-glomerular, glomerular and post-glomerular zones in fine cortical slices (100 μm thick). The counting live-time for each pixel was 100 s/step and the step size was 30 μm . Using these counting live-times, errors for each data by SR- μ XRF methodologies are < 0.1%.

2.3. Measurement and calibration of SR- μ XRF

For the evaluation of the resulting SR- μ XRF pixel spectra, the AXIL (Analysis of X-ray spectra by Iterative Least Squares) code was employed (Van Grieken and Markowicz, 1992). Finally, with the mathematical algorithm based on fundamental

parameters method, we were able to use the bulk concentration obtained by conventional wavelength dispersive XRF spectrometry (WDXRF) and the spatial mean value of the pixel SR- μ XRF intensities to obtain the calibration parameters for all elements. The slices of kidneys could not be considered infinitely thick, so we took the influence of sample thickness into account in the mathematical algorithm (Van Grieken and Markowicz, 1992). Mass attenuation coefficients were taken from McMaster et al. (1969), and energies of the emission lines were those compiled by Bearden and Burr (1967) and Bearden (1967) and Birks (1969). The white spectrum of the synchrotron x-ray beam measured by LNLS technicians was included in the code (Pérez et al., 2006b).

2.4. Statistics

The means and standard error were calculated for the data of at least three independent experiments. The Student's *t*-test was used to analyze the difference between the control and As-treated rats. In all cases, a $p < 0.05$ was considered to indicate a significant difference. Pearson's correlation coefficient (*R*-value) was calculated to determinate the degree of correlation between As and Cu distribution in the renal cortex. Four HE samples were obtained of each kidney. Each section was examined with a light microscope (40–200, BH2, Olympus) and histopathological

diagnosis was carried out independently by two of the authors (pathologist Cremonuzzi, D. and histology professor Bongiovanni, G.A.). The image was digitized using a high-resolution digital camera (Power Shot A460, Canon) and photomicrographs showing normal or injured tissue were selected as representative images.

3. Results and discussion

Related to excretory function, the kidneys in humans, animal models or naturally exposed fauna, are target organs for As accumulation and deleterious effects (Pomroy et al., 1980; Pérez et al., 2006a,b; ATSDR, 2007; Gerhardt et al., 1978; NRC, 1999; Meliker et al., 2007; Sasaki et al., 2007).

A comprehensive, interdisciplinary analysis was conducted in rats to study the effects of chronic As exposure on As retention in kidney. Histological and serum biochemistry alterations were correlated to cortical As/Cu co-distribution determined in renal slices by micro-X-Ray fluorescence methodologies.

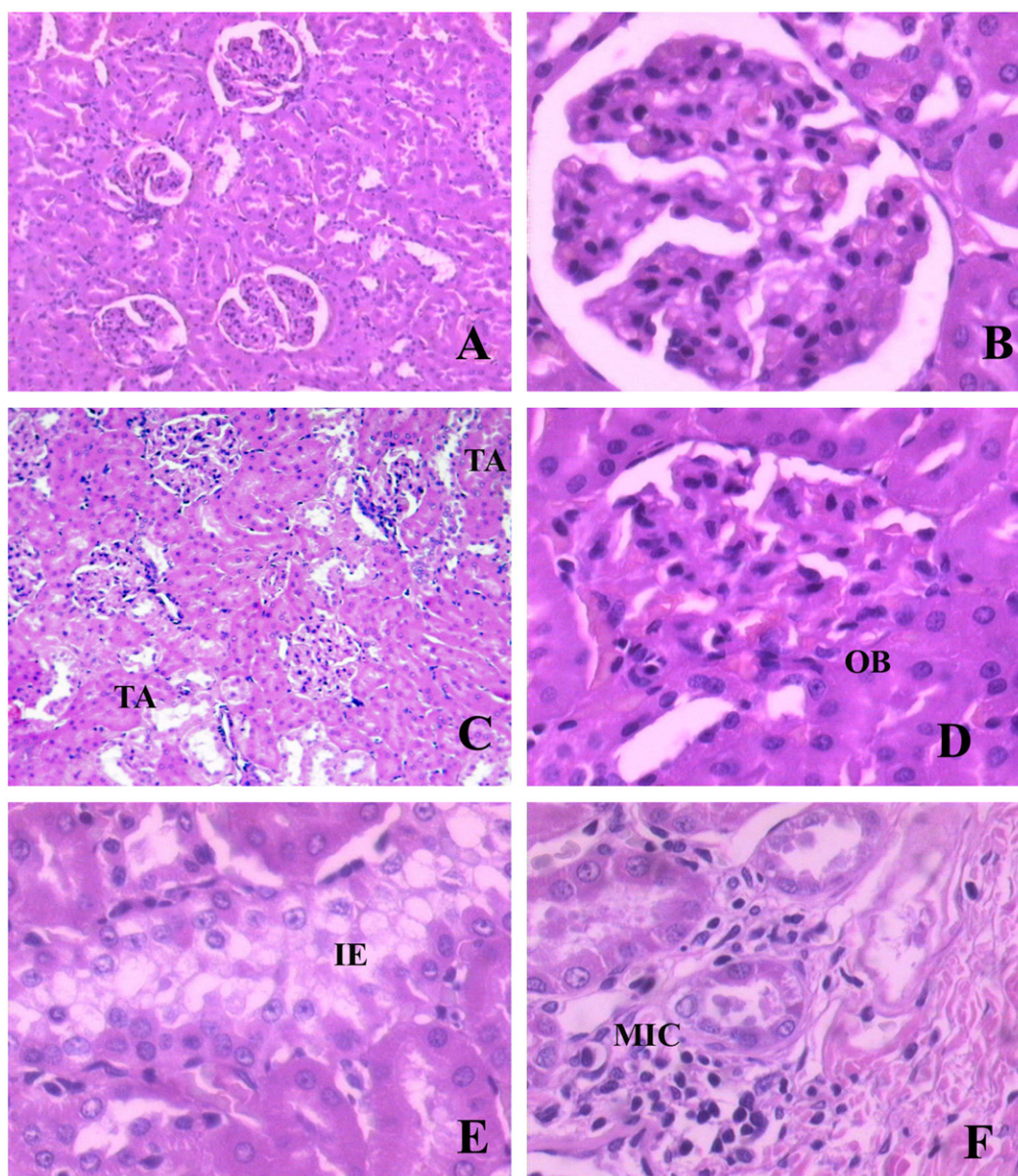


Fig. 1. Representative photomicrographs of rat renal cortex (HE). In controls, tubules and glomerulus show normal appearance. Tubular lumen and epithelial are preserved (A, 50 \times). The Bowman's space (BS) is preserved (B, 400 \times). After chronic As exposure for 60 days, panoramic view of renal cortex denotes tubular alterations (TA) and obliteration of Bowman's space (OB) (C, 50 \times). Magnified glomerulus is seen in D (400 \times). Following As exposure for 120 days, cortical tubules with enlargement of lumina and impaired epithelium (IE) are evident (E, 400 \times), while mononuclear inflammatory cells (MIC) are seen in the adjacent interstitium (dark nuclei in F, 400 \times).

3.1. Pathological examination

3.1.1. Macroscopic examinations

Feed consumption of exposed rats was similar to that of the controls. However, As presence decreased (around 20%) water intake in the first 4–5 days of exposure. Then, water intake was around 50 ml/day for all rats. Chronic As exposure from drinking water had no effect on animal body-weight gain during the 120 days of treatment and the weights of brain, spleen, kidneys, heart, pancreas, liver and testes of the animals were not significantly altered by chronic As. One spot (around 2 mm diameter) with necrotic aspect (dark brown) was seen in the spleen of one animal after 60 days of arsenite treatment. No behavioral changes were observed. All the animals survived As exposure.

3.1.2. Microscopic examinations

The light microscopic histological diagnosis of the kidney was normal at all time points in the control groups. Fig. 1 shows time-dependent degenerative changes in kidneys from As-exposed rats. Lesions observed in the kidneys were localized in the cortical area. At 60 days of treatment, more than 50% of the glomeruli were affected (Fig. 1), C. They showed expansion of the mesangial area with evident obliteration of Bowman's space and diminished capillary lumen. This alteration seems to be produced by an increase of mesangial cells and mesangial matrix (Fig. 1C and D). Varying degrees of epithelial cell damage were found in about 40% of tubular structures. This change was more severe at 120 days of treatment. Tubules were dilated, lined with a flattened epithelium (tubular cell vacuolation) and some exhibited acidophilic intraluminal casts (Fig. 1E). Mild interstitial inflammation with lymphocytes was observed (Fig. 1G). Using light microscopy and HE staining, no deposition of foreign material was observed. The tubular and interstitial impairment may be comparable to human tubular interstitial nephritis and the inflammatory cells may account for the increased production of various pro-inflammatory cytokines found in chronically As-exposed mice, where a significant role of cytokines in As-induced kidney injury had been postulated (Liu et al., 2000).

3.2. Biochemical alterations

An increased blood urea nitrogen (BUN)-to-creatinine ratio due to abnormal tubular reabsorption has been found to be predictive of pre-renal failure (Morgan et al., 1977). In this study, indicating arsenic-related kidney dysfunction, the BUN/creatinine ratio was significantly increased after following 60 days of As exposure (Fig. 2). Consistent with the literature (Nabi et al., 2005; Wang et al., 2006), an up to 40% reduction in plasma creatinine values was observed after 60 days of As intake (not shown). These laboratory tests could be used as early indicators of tubular cell injuries and dysfunction.

In summary, long-term As exposure induces morphological and functional tubular deterioration. It is clear that the nephrotoxicity of this agent is due, in part, to the fact that urinary elimination is a major route of excretion from the body. Renal tubules are especially sensitive because of their reabsorptive activity.

3.3. As and Cu distribution in renal slides

Arsenic exposure induces As and Cu retention in kidney of several species in a time- and dose-dependent manner (Schmolke et al., 1992; Hunder et al., 1999; Wang et al., 2006; Pérez et al., 2006b). However, the liver, another As target organ, accumulates As but the copper level is not affected (Pérez et al., 2006a, 2008).

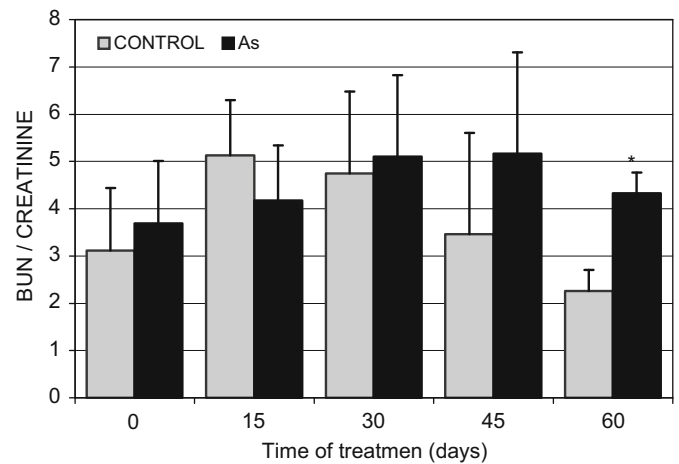


Fig. 2. Effect of chronic As exposure on blood urea nitrogen/creatinine ratio levels. Wistar rats were fed 100 ppm arsenite in drinking water for 60 days. Data are the means \pm SEM of two experiments. *Significantly different from control.

This suggests a particular relationship between arsenic and copper in renal tissue. To gain insight into the spatial distribution of As and Cu in kidney, and correlate this with histological and physiological evidence of injury, maps of As and Cu concentration were obtained with micro-X-ray fluorescence spectrometry by synchrotron radiation (SR- μ XRF). When 2-mm-thick kidney slices were scanned with a collimated white synchrotron spectrum (300 μ m \times 300 μ m), an unambiguous cortical accumulation of As and Cu was found. In Fig. 3, 3-D maps of As and Cu shows a 100% co-distribution in the cortical zone (Fig. 3, As-Cu_A). These results are in agreement with our own previous report (Pérez et al., 2006b) as well as with others obtained by indirect and destructive methodologies (Schmolke et al., 1992). Furthermore, a functional relationship between As and Cu has been suggested with respect to their retention in the kidney after arsenite administration (Ademuyiwa and Elsenhans, 2000). The toxicity of both elements has been unambiguously demonstrated in a variety of experimental and epidemiological studies. Interestingly, both elements are involved in the generation of reactive oxygen species (ROS) in cells. In this regard, Cu toxicity can result in significant oxidative stress and subsequent tissue damage (Uriu-Adams and Keen, 2005). So, a renal parenchyma accumulation of these elements may be critical for that organ. As shown in Fig. 3, As_{As} arsenic was detected in the cortical and paracortical areas, and tubular lesions were the major hallmark in the kidney of arsenic-treated animals. The cortical co-distribution of As-Cu supports the hypothesis of a tubular accumulation and an involvement of the As-Cu relationship in the arsenic-associated nephrotoxicological process. In order to analyze these hypotheses, the As and Cu concentrations in pre-glomerular, glomerular and post-glomerular zones were determined in 100- μ m-thick renal cortical slices by SR- μ XRF using a focused white beam (30 μ m \times 30 μ m). Homogeneous distribution of Cu was found in the renal cortex from control animals (average: 36.17 \pm 9.77 ppm). In contrast, both elements accumulated and co-localized in the peri-glomerular zone in a time- and concentration-dependent manner, indicating a closed As-Cu position (Fig. 4). Thus, after 60 days, As and Cu accumulations in the peri-glomerular zone were 197.71 \pm 18.48 and 209.61 \pm 26.35 ppm (average of values in curve, respectively) and 138.12 \pm 13.60 and 124.41 \pm 11.87 ppm (average, respectively) in the glomerular zone). After 120 days, the accumulation of As and Cu was increased in the peri-glomerular zone (average: 374.27 \pm 37.69 and 385.55 \pm 39.48 ppm, respectively), while only the As concentration increased in

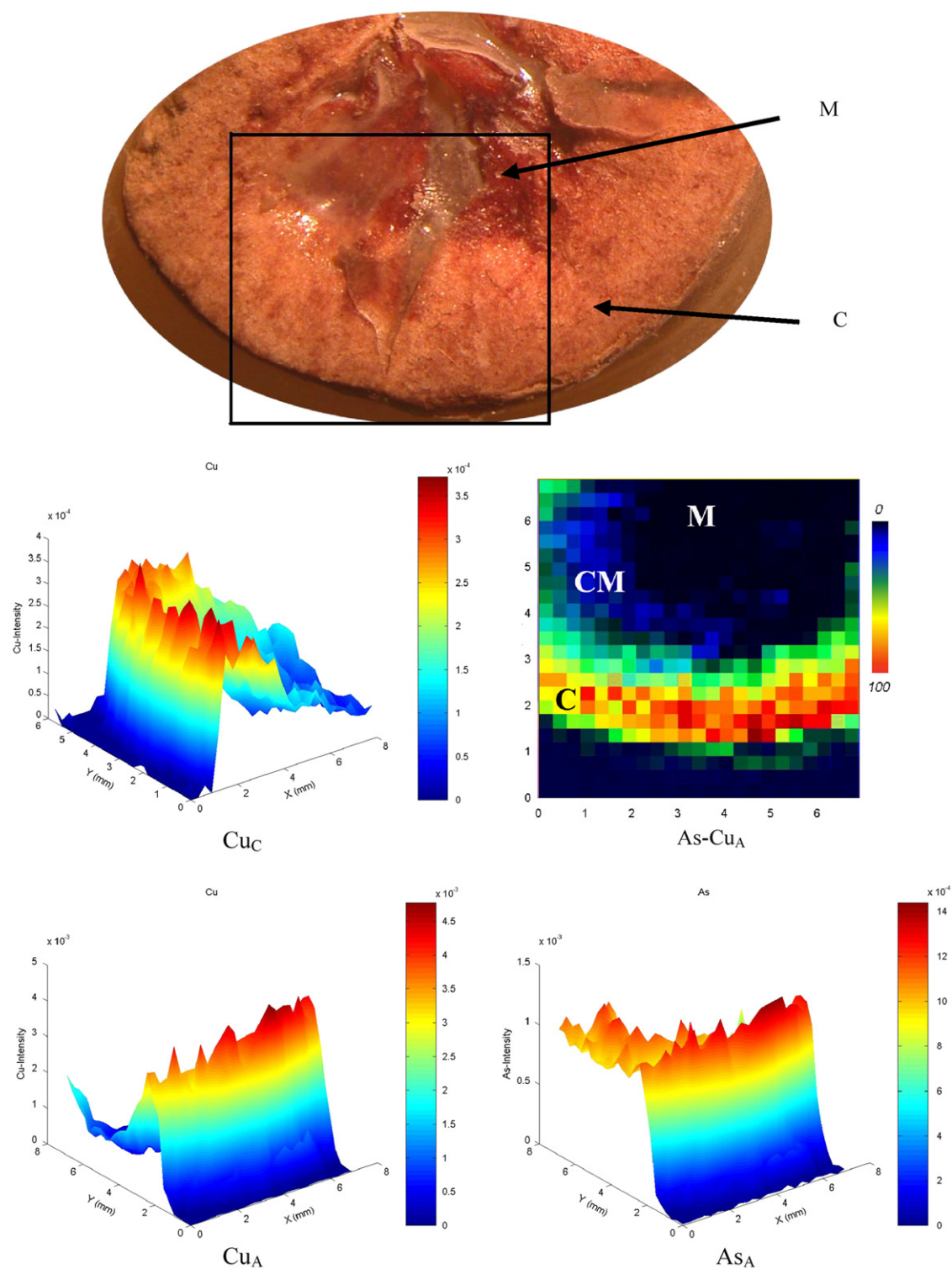


Fig. 3. Representative 3-D maps of As and Cu distribution in kidney. x - y axes represent spatial distribution; z -axis represents fluorescent intensity (FI). 8×8 mm areas in slices of 2 mm thick were scanned with a $300 \mu\text{m} \times 300 \mu\text{m}$ collimated white synchrotron spectrum (upper photo). M: medulla, CM: cortico-medullar zone, C: renal cortex. Cu_C: Cu distribution in kidney of control rats (maximum FI = 3.75×10^{-4}). As-Cu_A: As-Cu co-distribution in renal cortex of 60 days As-treated group as percentage of fingerprinting. Cu_A and As_A: As and Cu distribution in kidney of 60 days As-treated group (maximum FI = 4.75×10^{-3} and 14.25×10^{-4} , respectively). Note that FI is not linearly proportional to concentration between different elements (Pérez et al., 1999).

the glomerular zone (average: 503.89 ± 64.06 ppm). Cu concentration in the glomerular zone was 148.23 ± 13.20 ppm (average).

The strong linear correlation (Pearson's correlation coefficient between 0.81 and 0.95) between As and Cu curves of concentration

shown in Fig. 4, together with the pattern of distribution in the peri-glomerular zone after arsenite administration, provide support for the hypothesis of As-Cu interaction in the renal cortex. Although we cannot completely rule out an indirect As-Cu interaction by binding to the same molecular target such as

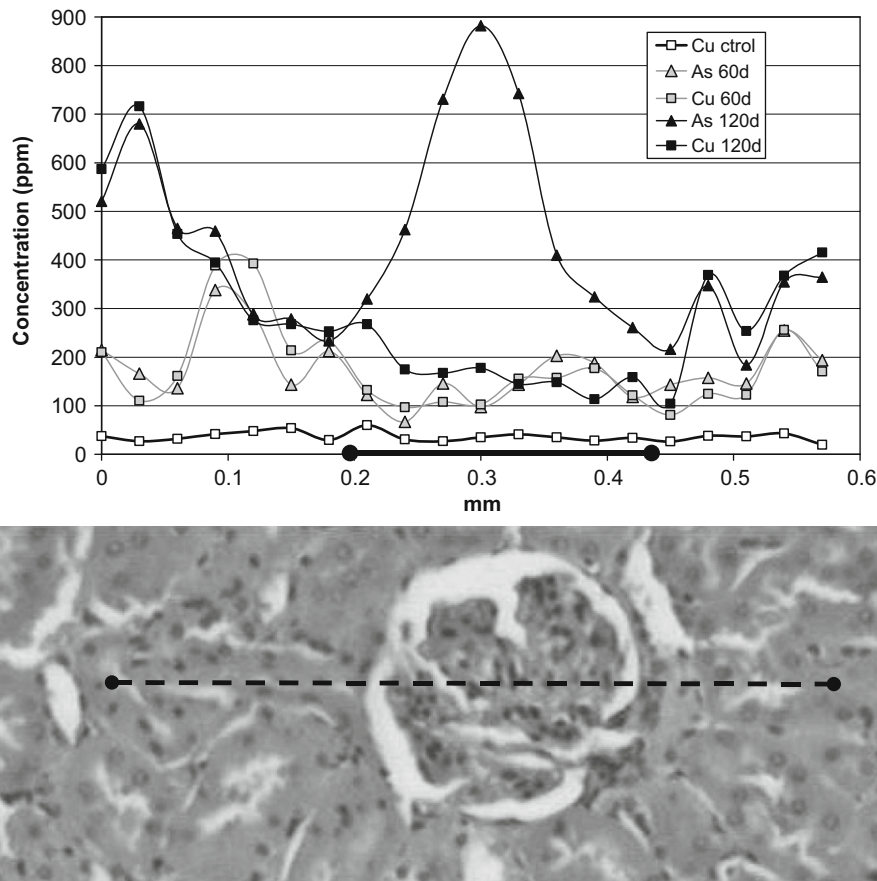


Fig. 4. A transect line of 20 points was obtained by measuring K_{α} X-ray fluorescence intensity across pre-glomerular, glomerular and post-glomerular zones from 100- μ m-thick renal slices (see material and methods). The thick line on the x-axis denotes glomerulus position. The values are the average of six determinations in different experiments. For clearer presentation, the error bars ($< 10\%$ in every cases) were omitted. Below, a representative photomicrograph of scanned zones.

metallothionein or a cellular target such as mitochondria (Cui and Okayasu, 2008; Liu et al., 2005), we conclude that, in the rat model, As–Cu interaction resulting in tubular (more than glomerular) accumulation may be an important component of the morphologic and physiologic renal alterations involved in arsenic-induced nephrotoxicological processes. Perhaps more significant is the fact that these observations were made using non-destructive methodologies.

Although, the relationship between As–Cu co-distribution in renal cortex and tubular injury was shown here in rats, renal As–Cu interaction is not restricted to these animals (Hunder et al., 1999; Wang et al., 2006). Additionally, chromium copper arsenate (CCA) administration results in a marked decrease of the kidney's ability to eliminate its components simultaneously as well as a higher nephrotoxicity (tubular necrosis) than As administration, evidencing a possible synergetic effect (Matos et al. (2009)). No studies were located regarding Cu determination in human kidneys after chronic exposure to inorganic arsenicals. However, methylated As species are excreted more rapidly than unmethylated species and only inorganic arsenic is involved in As–Cu interaction (Marafante et al., 1987; Bogdan et al., 1994; Hunder et al., 1999). So, As retention in the human kidney after long-term exposure could be accompanied by arsenic-associated Cu retention. This would be found particularly in children, whose metabolism of arsenic is less efficient than that in adults (Concha et al., 1998). Thus, additional studies are needed to establish the role of As–Cu interaction in the arsenic-associated nephropathological process.

Acknowledgments

This study was supported by funds provided by Brazilian Synchrotron Light Laboratory (LNLS-ABTLuS D09B-XRF-5185/2006 and 6450/2007), CONICET and Ministry of Science and Technology of Córdoba, Argentina (Res. 969/2005). The authors would like to thank Joss Heywood for the English revision (native speaker).

References

- Ademuyiwa, O., Elsenhans, B., 2000. Time course of arsenite-induced copper accumulation in rat kidney. *Biol. Trace Elem. Res.* 74 (1), 81–92.
- ATSDR (Agency for Toxic Substances and Disease Registry)2007. Division of Toxicology and Environmental Medicine, Department of Health and Human Services USA, Toxicological Profile for Arsenic. www.atsdr.cdc.gov/toxprofiles/tp2.thml.
- Bearden, J.A., 1967. X-Ray wavelengths. *Rev. Mod. Phys.* 39, 78–124.
- Bearden, J.A., Burr, A.F., 1967. Reevaluation of X-ray atomic energy levels. *Rev. Mod. Phys.* 39, 125–142.
- Birks, L.S., 1969. In: *Handbook of Spectroscopy*. CRC Press, Cleveland, OH.
- Bogdan, G.M., Sympayo-Reyes, A., Aposhian, H.V., 1994. Arsenic binding proteins of mammalian systems. I. Isolation of three arsenite binding proteins of rabbit liver. *Toxicology* 93, 175–193.
- Bongiovanni, G., Soria, E.A., Eynard, A.R., 2007. Effects of the plant flavonoids silymarin and quercetin on arsenite induced oxidative stress in CHO K1 cells. *Food Chem. Toxicol.* 45 (6), 971–976.
- Concha, G., Nermell, B., Vahter, M.V., 1998. Metabolism of inorganic arsenic in children with chronic high arsenic exposure in northern Argentina. *Environ. Health Perspect.* 106, 355–359.
- Cui, X., Okayasu, R., 2008. Arsenic accumulation, elimination, and interaction with copper, zinc and manganese in liver and kidney of rats. *Food Chem. Toxicol.* 46 (12), 3646–3650.

- Figuroa, R.G., Bongiovanni, G.A., 2008. Comparison between different methods in dust air on polycarbonate filters analysis by XRF using synchrotron radiation. *Av. anal. téc. rayos x* 14, 139–145.
- Gerhardt, R.E., Hudson, J.B., Rao, R.N., Sobel, R.E., 1978. Chronic renal insufficiency from cortical necrosis induced by arsenic poisoning. *Arch. Intern. Med.* 138, 1267–1269.
- Hunder, G., Schaper, J., Ademuyiwa, O., Elsenhans, B., 1999. Species differences in arsenic-mediated renal copper accumulation: a comparison between rats, mice and guinea pigs. *Hum. Exp. Toxicol.* 18 (11), 699–705.
- Liu, J., Liu, Y., Goyer, R.A., Achanzar, W., Waalkes, M.P., 2000. Metallothionein-1/II null mice are more sensitive than wild-type mice to the hepatotoxic and nephrotoxic effects of chronic oral or injected inorganic arsenicals. *Toxicol. Sci.* 55, 460–467.
- Liu, S.X., Davidson, M.M., Tang, X., Walker, W.F., Athar, M., Ivanov, V., Hei, T.K., 2005. Mitochondrial damage mediates genotoxicity of arsenic in mammalian cells. *Cancer Res.* 65, 3236–3242.
- Marafante, E., Vahter, M., Norin, H., Envall, J., Sandstrom, M., Christakopoulos, A., Ryhage, R., 1987. Biotransformation of dimethylarsinic acid in mouse, hamster and man. *J. Appl. Toxicol.* 7, 111–117.
- Matos, R.C., Vieira, C., Morais, S., Pereira, M.L., Pedros, J., 2009. Nephrotoxicity effects of the wood preservative chromium copper arsenate on mice: Histopathological and quantitative approaches. *J. Trace Elem. Med. Biol.* 23, 224–230.
- McMaster, W.H., Kerr del Grande, N., Mallet, J.H., Hubbell J., 1969. Compilation of x-ray cross section, Report UCRL 50174, Section 2, Rev 1. Lawrence Livermore National Laboratory, Livermore, CA.
- Meliker, J.R., Wahl, R.L., Cameron, L.L., Nriagu, J.O., 2007. Arsenic in drinking water and cerebrovascular disease, diabetes mellitus, and kidney disease in Michigan: a standardized mortality ratio analysis. *Environ. Health* 6.
- Morgan, D.B., Carver, M.E., Payne, R.B., 1977. Plasma creatinine and urea: creatinine ratio in patients with raised plasma urea. *Br. Med. J.* 2 (6092), 929–932.
- Nabi, A.H., Rahman, M.M., Islam, L.N., 2005. Evaluation of biochemical changes in chronic arsenic poisoning among Bangladeshi patients. *Int. J. Environ. Res. Public Health* 2 (3–4), 385–393.
- NRC, 1999. Arsenic in the Drinking Water. National Research Council, National Academy Press, Washington, DC.
- Parrish, A.R., Zheng, X.H., Turney, K.D., Younis, H.S., Gandolfi, A.J., 1999. Enhanced transcription factor DNA binding and gene expression induced by arsenite or arsenate in renal slices. *Toxicol. Sci.* 50, 98–105.
- Peraza, M.A., Cromey, D.W., Carolus, B., Carter, D.E., Gandolfi, A.J., 2006. Morphological and functional alterations in human proximal tubular cell line induced by low level inorganic arsenic: evidence for targeting of mitochondria and initiated apoptosis. *J. Appl. Toxicol.* 26 (4), 356–367.
- Pérez, C.A., Radtke, M., Sanchez, H.J., Tolentino, H., Neuenschwander, R.T., Barg, W., Rubio, M., Bueno, M.I.S., Raimundo, I.M., Rohwedder, J.J.R., 1999. Synchrotron radiation X-Ray fluorescence at the LNLS: beamline instrumentation and experiments. *X-Ray Spectrom.* 28 (5), 320–326.
- Pérez, R.D., Rubatto Birri, P.N., Pérez, C.A., Rubio M., Bongiovanni, G.A., 2006a. Multielemental mapping and arsenic determination in organs of rats by SR μ XRF. LNLS Activity Report 2005.
- Pérez, R.D., Rubio, M., Pérez, C.A., Eynard, A.R., Bongiovanni, G.A., 2006b. Study of the effects of chronic arsenic poisoning on rat kidney by means of synchrotron microscopic X ray fluorescence analysis. *X-Ray Spectrom.* 35 (6), 352–358.
- Pérez, R.D., Rubatto Birri, P.N., Rubio, M., Pérez, C.A., Bongiovanni, G.A., 2008. Microanálisis por fluorescencia de rayos X por radiación Síncrotron de hígado y páncreas de ratas bajo exposición crónica de arsénico. *Av. anal. téc. rayos x* 14, 283–288.
- Pomroy, C., Charbonneau, S.M., McCullough, R.S., Tam, G.K.H., 1980. Human retention studies with ^{74}As . *Toxicol. Appl. Pharmacol.* 53, 550–556.
- Rubatto Birri, P.N., Pérez, R.D., Pérez, C.A., Rubio, M., Eynard, A.R., Bongiovanni, G.A., 2007. Distribución de Na, P, S, Cl, K, Ca, Mn, Fe, Cu, Zn, As y Br en órganos de rata y marcadores de toxicidad tras ingesta crónica de agua con arsénico. (Abs.). *Acta Toxicol. Arg.* 15 (Suppl.), 68.
- Rubio, M., Pérez, R.D., Pérez, C.A., Eynard, A.R., Bongiovanni, G.A., 2008. Synchrotron microscopic x-ray fluorescence analysis of the effect of chronic arsenic exposure in rat brain. *Radiat. Phys. Chem.* 77 (1), 1–8.
- Sasaki, A., Oshima, Y., Fujimura, A., 2007. An approach to elucidate potential mechanism of renal toxicity of arsenic trioxide. *Exp. Hematol.* 35, 252–262.
- Schmolke, G., Elsenhans, B., Eltehami, C., Forth, W., 1992. Arsenic-copper interaction in the kidney of the rat. *Hum. Exp. Toxicol.* 11 (5), 315–321.
- Schnellmann, R.G., Kelly, K.J., 1999. Pathophysiology of nephrotoxic acute renal failure. In: Robert W. Schrier (Series Editor), *Atlas of Diseases of the Kidney*. vol. 1, Tomas Berl, Joseph V. Bonventre (Eds.). Blackwell Publishing (Chapter 15).
- Soria, E.A., Goleniowski, M.E., Cantero, J.J., Bongiovanni, G.A., 2008. Antioxidant activity of different extracts of Argentinean medicinal plants against arsenic-induced toxicity in renal cells. *Hum. Exp. Toxicol.* 27, 341–346.
- Tapio, S., Grosche, B., 2006. Review: arsenic in the etiology of cancer. *Mut. Res.* 612, 215–246.
- Uriu-Adams, J.Y., Keen, C.L., 2005. Review: copper, oxidative stress, and human health. *Mol. Aspects Med.* 26, 268–298.
- Vahter, M., Akesson, A., Lidén, C., Ceccatelli, S., Berglund, M., 2007. Gender differences in the disposition and toxicity of metals. *Environ. Res.* 104 (1), 85–95.
- Van Grieken, R.E., Markowicz, A.A., 1992. In: *Handbook of X-Ray Spectrometry*. Marcel Dekker Inc. Publisher, New York/Handbook of X-Ray Spectrometry. Marcel Dekker Inc. Publisher, New York.
- Wang, L., Xu, Z.R., Jia, X.Y., Han, X.Y., 2006. Effects of dietary arsenic levels on serum parameters and trace mineral retentions in growing and finishing pigs. *Biol. Trace Elem. Res.* 113 (2), 155–164.
- Yoshida, T., Yamauchi, H., Sun, G.F., 2004. Chronic health effects in people exposed to arsenic via the drinking water: dose–response relationships in review. *Toxicol. Appl. Pharm.* 198, 243–252.